

Resourcefulness of non-classical continuous-variable quantum gates

Massimo Frigerio, Antoine Debray, Nicolas Treps, and Mattia Walschaers

Laboratoire Kastler Brossel, Sorbonne Université, CNRS, ENS-Université PSL, Collège de France, 4 place Jussieu, F-75252 Paris, France
March 11, 2025

In continuous-variable quantum computation, identifying key elements that enable a quantum computational advantage is a long-standing issue. Starting from the standard results on the necessity of Wigner negativity, we develop a comprehensive and versatile approach in which the techniques of (s)-ordered quasiprobabilities are exploited to identify the contribution of each quantum gate to the potential achievement of quantum computational advantage. This is achieved by means of an analysis of the so-called transfer function, allowing us to highlight the resourcefulness of a gate set. As such this technique can be straightforwardly applied to current continuous-variables quantum circuits, while also constraining the tolerable amount of losses above which any potential quantum advantage can be ruled out. We use (s)-ordered quasiprobability distributions on phase-space to capture the non-classical features in the protocol, and focus our technique entirely on the ordering parameter s . This allows us to highlight the resourcefulness and robustness to loss of a universal set of unitary gates comprising three distinct Gaussian gates, and a fourth one, the cubic gate, providing important insight on the role of non-Gaussianity.

1 Introduction

Ever since Shor's algorithm [1] promised an exponential speed-up in the factorisation of prime numbers, quantum computing has captivated the scientific community. The laws and logic behind quantum physics make it possible to solve certain highly specific problems much more efficiently than what could be achieved with classical devices. While it is not unreasonable to expect that quantum computers hold huge potential as a new computational framework, so far actual algorithmic design have only scratched the surface [2].

A bit over a decade ago, a new approach to study the question of the computational advantage of quantum devices over classical ones was introduced. Spe-

Mattia Walschaers: mattia.walschaers@lkb.upmc.fr

cific protocols such as boson sampling [3], IQP [4], and random circuit sampling [5], were proposed as candidates for reaching a provable quantum computational advantage. The foundations of these works within computational complexity theory [6, 7] separates them from earlier works on quantum speed-ups in the sense that there are strong arguments to suggest that these protocols cannot be simulated efficiently by any classical algorithm. These works have ultimately led to a series of experiments claiming to have reached such a quantum computational advantage [8–11].

In the field of photonic quantum computation, the boson sampling protocol and its many variations [12–16] have drawn much attention. The race for a quantum computational advantage quickly imposed the question: when do noise and experimental imperfections make a setup efficiently simulable on a classical computer? This has led to some very concrete results exploiting the fine details of boson sampling [17–20] and gaussian boson sampling [21–25] setups. Furthermore, this sparked research activities on the simulation of photonic sampling problems in a more general context.

This more general line of research can be seen as a series of attempts to translate and generalise the Gottesman-Knill theorem [26] for bosonic systems. The first such generalisation dates back to the early days of continuous-variable quantum information processing, and it showed simply that a setup involving exclusively Gaussian states, operation, and measurements can be efficiently simulated [27]. For a highly ideal setup with pure states, unitary gates, and projective measurements, Hudson's theorem [28, 29] teaches us that these Gaussian elements are the only ones that are described by a fully positive Wigner function [30]. When more general sampling setups are considered, allowing states to be mixed, measurements can be general positive-operator valued measures (POVMs), and gates to be described by general channels, it turns out that this positivity of the Wigner function is the element that makes a system efficiently simulable [31, 32]. In other words, the existence for negative regions in the Wigner functions that describe the system is a key resource for reaching a quantum computational advantage.

While such Wigner negativity might be a necessary resource, it clearly is not a sufficient one [33].

A series of recent works has used tools from bosonic codes to completely challenge the paradigm of Wigner negativity as a crucial resource [34, 35], relying instead on discrete-variable resources that come from the qubits that bosonic codes are encoding [36]. However, these sufficient resources may turn out to be more demanding than necessary. In this regard, other works have searched for new necessary resources for reaching a quantum computational advantage, leading to the identification of stellar rank and some non-Gaussian type of entanglement as key ingredients [37]. Other approaches have aimed to generalise the results of Wigner negativity to more general phase-space representations [20, 38].

Most of these recent results have focused primarily on the resources that are present in the initial states and/or the measurements. The resourcefulness of the operations that are implemented in between (typically quantum gates) have not received much attention. In works such as [20, 34] these operations are limited to a very specific class of circuits, or one directly considers measurements on some generic state as in [37]. These works therefore assume, either explicitly or implicitly, that a straightforward approach can be taken when addressing big multimode channel connecting input states to measurements. This is in strong contrast with [31], where a lot of attention is devoted to the development of a Markov chain model to simulate the action of a sequence of few-mode quantum channels. This can effectively be understood as a hidden-variable model for quantum computing which allows, at least in principle, to study a very wide set of operations.

In the present work, we build upon the ideas of [20], going beyond their results by arguing that the ordering parameters can be chosen in an optimal way that also allows us to treat quantum gates in a decoupled, independent manner, thereby precisely identifying the sources of quantum computational advantage within a circuit. By introducing an algorithmic approach to derive the best decomposition of a quantum circuit in terms of (s) -ordered quasiprobability distributions, we demonstrate the significant insights that the framework of [20] can yield. It is worth highlighting that our approach effectively looks for an optimal hidden variable model for the computation, by optimizing the choice of s ordering parameters in the representation of subsequent layers of operations. Moreover, this algorithm allows us to effectively deal with specific amounts of losses or noise at precise points in the circuit. Even if we find that a certain protocol is impossible to simulate, because no appropriate (s) -parameters can be found, our approach allows us to identify how much losses or noise can be tolerated before the setup can be efficiently simulated.

The key point of our work lies in the second part, sections 4 and 5, where we devote attention to specific types of quantum gates and channels that are highly

relevant in photonic quantum computing. Through an examination of their respective transfer functions, and the manner in which each function fits within the decoupled approach outlined in section 3, it becomes possible to pinpoint the precise sources of quantum computational advantage within a circuit, or, conversely, where such advantage is crucially lost. This notably allows us to understand the role of squeezing operations, photon addition and subtraction, and deterministic non-Gaussian gates such as the cubic phase gate in reaching a quantum computational advantage.

2 Phase-space Representations

2.1 (s) -ordered representations of states and observables

The main theoretical tool on which our results will rely consists in (s) -ordered quasiprobability distributions (quasi-PDF) on phase-space. Let us consider a Fock space of M bosonic modes, each associated with its pair of creation and annihilation operators $\hat{a}_j^\dagger, \hat{a}_j$ such that $[\hat{a}_j, \hat{a}_k^\dagger] = \delta_{jk}$. We will denote by $\hat{\mathbf{a}} = (\hat{a}_1, \dots, \hat{a}_M)$ the corresponding vector of operators. For a bounded operator \hat{O} on such space, and for any real number $s \in [-1, 1]$, we then define the (s) -ordered phase-space representation [30, 39]

$$W_{\hat{O}}^{(s)}(\boldsymbol{\alpha}) = \int_{\boldsymbol{\xi} \in \mathbb{C}^M} \frac{d^{2M} \boldsymbol{\xi}}{\pi^{2M}} \chi_{\hat{O}}^{(s)}(\boldsymbol{\xi}) e^{\boldsymbol{\alpha} \boldsymbol{\xi}^\dagger - \boldsymbol{\xi} \boldsymbol{\alpha}^\dagger}, \quad (1)$$

where $\boldsymbol{\xi}, \boldsymbol{\alpha} \in \mathbb{C}^M$ are complex vectors. The (s) -ordered characteristic function $\chi_{\hat{O}}^{(s)}(\boldsymbol{\xi})$ is defined by

$$\chi_{\hat{O}}^{(s)}(\boldsymbol{\xi}) = \text{Tr} \left[\hat{O} \hat{D}(\boldsymbol{\xi}, s) \right], \quad (2)$$

with $\hat{D}(\boldsymbol{\xi}, s)$ the (s) -ordered displacement operator $\hat{D}(\boldsymbol{\xi}, s) = \hat{D}(\boldsymbol{\xi}) e^{\boldsymbol{\xi} s \boldsymbol{\xi}^\dagger / 2}$, which is a generalisation of the standard M -modes displacement operator $\hat{D}(\boldsymbol{\xi}) = \exp\{\boldsymbol{\xi} \hat{\mathbf{a}}^\dagger - \boldsymbol{\xi}^\dagger \hat{\mathbf{a}}\}$. These (s) -ordered representations are useful tools to study CV quantum systems due to the identity [30, 39]

$$\text{Tr} \left[\hat{O}_1 \hat{O}_2 \right] = \int_{\boldsymbol{\alpha} \in \mathbb{C}^M} \frac{d^{2M} \boldsymbol{\alpha}}{\pi^M} W_{\hat{O}_1}^{(-s)}(\boldsymbol{\alpha}) W_{\hat{O}_2}^{(s)}(\boldsymbol{\alpha}). \quad (3)$$

We emphasize the requirement of pairing a quasiprobability distribution with parameter s with one with parameter $-s$. As indicated in fig. 1, the higher the value of s , the more singular the distributions. Vice-versa, lower values of s indicate more regular phase-space representations.

Phase-space representations are often used to characterise quantum states, in which case we choose \hat{O} in eq. (1) to be the density matrix $\hat{\rho}$. The (s) -ordered phase-space representation then becomes a quasiprobability distribution, meaning that it is normalised, but

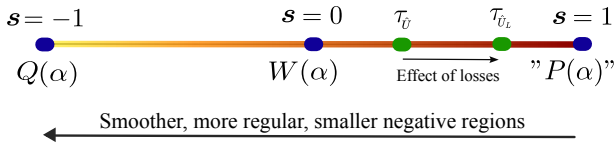


Figure 1: The range of values of the (s) -parameter. The values corresponding to the Q -, P -, and Wigner function are highlighted. We also visually represent the effect of eq. (18), which describes how losses drive the nonclassical parameter closer to one.

not necessarily positive. For the case $s = 0$, we recover the Wigner function. For $s = -1$, instead, we have the Husimi Q -function, which is always non-negative and normalised to 1, being a proper probability density function (PDF) associated with a non-projective measurement onto coherent states. At the opposite hand, for $s = 1$, the integral won't always converge to some regular function and the result is instead defined as a distribution, i.e. a linear functional on a space of test functions, and it bears the name of Glauber's P -representation.

Importantly, it is possible to transform a (s) -ordered representation into a (s') -ordered representation with $s' < s$ by convoluting it with a Gaussian function:

$$W_{\hat{O}}^{(s')}(\alpha) = \frac{2}{s-s'} \int_{\beta \in \mathbb{C}^M} \frac{d^2\beta}{\pi^2} e^{-\frac{2|\alpha-\beta|^2}{s-s'}} W_{\hat{O}}^{(s)}(\beta). \quad (4)$$

Clearly then, $W_{\hat{O}}^{(s')}(\alpha)$ will be more regular than $W_{\hat{O}}^{(s)}(\alpha)$ for $s' < s$ [40]. If we are dealing with a quantum state, $\hat{O} = \hat{\rho}$, with a negative Wigner function ($s = 0$), looking for the highest value of $s' < 0$ such that $W_{\hat{\rho}}^{(s')}$ is a PDF amounts to finding the narrowest Gaussian kernel that will erase all the negative regions in the original Wigner function. As such, it is a means of quantifying Wigner negativity, referred to as the non-classical depth, which will be addressed in the following paragraph. Unlike most common measures of Wigner negativity, such as the negativity volume, though, it also takes into account how the negative regions are shaped in phase-space: a very elongated negativity region would require a much broader Gaussian to be fully cancelled, when compared to another region with the same negative volume but a more symmetric shape. To quantify this idea, we can use the negativity volume:

$$\mathcal{N}^{(s)}(\hat{\rho}) = \int_{\alpha \in \mathbb{C}^M} d^{2M} \alpha |W_{\hat{\rho}}^{(s)}(\alpha)| - 1. \quad (5)$$

Combining with eq. (4) and standard integral inequalities for absolute values we directly find that

$$\mathcal{N}^{(s')}(\hat{\rho}) \leq \mathcal{N}^{(s)}(\hat{\rho}) \quad \text{for all } s' \leq s. \quad (6)$$

More generally, also for Wigner-positive states, we can define τ as the maximal value for which $\mathcal{N}^{(\tau)}(\hat{\rho}) = 0$,

and thus $W_{\hat{\rho}}^{(\tau)}(\alpha)$ is a PDF. Given that the Husimi Q -function is obtained by projecting $\hat{\rho}$ onto coherent states, it is clear that such a $\tau \geq -1$ always exists. This value τ defines the *nonclassical depth* [41] of the state $\hat{\rho}$:

$$\mathfrak{t}[\hat{\rho}] := \frac{1-\tau}{2} \quad (7)$$

All non-Gaussian pure states have nonclassical depth $\mathfrak{t} = 1$ (meaning that only their Q -function is a PDF). For Gaussian states, since they have positive Wigner functions, $\mathfrak{t} \leq 1/2$, and for the particular case of coherent states we obtain $\mathfrak{t} = 0$. The latter are the only pure states whose P -function is a PDF, thus they are commonly referred to as the only classical pure state. The nonclassical depth can be employed as a measure of nonclassicality of quantum states and is particularly informative for mixed states and noisy quantum processes.

Up to now, we have only considered the case with one single ordering parameter. However, dealing with multimode states, it is much richer to define the (\mathbf{s}) -ordered phase-space representation such that $\mathbf{s} = \text{diag}(s_1, s_2, \dots, s_M)$ is a diagonal matrix, in such a way that each mode has its own independent ordering parameter, instead of choosing a single ordering parameter for all modes. This simply boils down to replacing $\hat{D}(\boldsymbol{\xi}, s)$ with $\hat{D}(\boldsymbol{\xi}, \mathbf{s}) = \hat{D}(\boldsymbol{\xi}) e^{\boldsymbol{\xi} \mathbf{s} \boldsymbol{\xi}^\dagger / 2}$ in eq. (2). Consequently, the (\mathbf{s}) -ordered representation of any operator \hat{O} is designated by $W_{\hat{O}}^{(\mathbf{s})}$. For $\mathbf{s} = -\mathbb{1}_M$, $\mathbf{s} = 0_M$ and $\mathbf{s} = \mathbb{1}_M$ one finds respectively the Husimi Q -function, the Wigner function and the Glauber-Sudarshan P -function.

2.2 (s) -ordered representations of quantum operations

We first consider a generic quantum optical scheme: M input bosonic modes, described by a density operator $\hat{\rho}_{in}$, are processed by a trace-preserving completely positive (CPTP) quantum channel \mathcal{E} . The overall output state $\hat{\rho}_{out} = \mathcal{E}(\hat{\rho}_{in})$ is then measured by a *factorized* POVM $\hat{\Pi}_{\mathbf{x}}$, \mathbf{x} being the generic label for each possible measurement result. It was shown in [20] that the probability to obtain the outcome \mathbf{x} is given by

$$p(\mathbf{x}) = \iint_{\alpha, \beta \in \mathbb{C}^M} \pi^M d^{2M} \alpha d^{2M} \beta W_{\rho_{in}}^{(s')}(\alpha) \times \Lambda_{\mathcal{E}}^{(-s', s)}(\alpha, \beta) W_{\hat{\Pi}_{\mathbf{x}}}^{(-s)}(\beta). \quad (8)$$

where $\Lambda_{\mathcal{E}}^{(s', s)}(\alpha, \beta)$ is the (s', s) -ordered transfer function of \mathcal{E} , defined as:

$$\Lambda_{\mathcal{E}}^{(s', s)}(\alpha, \beta) = \iint_{\zeta, \xi \in \mathbb{C}^M} d^{2M} \zeta d^{2M} \xi e^{\beta \zeta^\dagger - \zeta \beta^\dagger + \xi \alpha^\dagger - \alpha \xi^\dagger} \times e^{\zeta \mathbf{s} \zeta^\dagger / 2 + \xi \mathbf{s}' \xi^\dagger / 2} \text{Tr} \left[\mathcal{E}(\hat{D}^\dagger(\boldsymbol{\xi})) \hat{D}(\boldsymbol{\zeta}) \right]. \quad (9)$$

As such, the transfer function $\Lambda_{\mathcal{E}}^{(s',s)}(\alpha, \beta)$ is a phase-space representation of the trace preserving quantum operation \mathcal{E} . Moreover, the transfer function in eq. (9) comes with an interesting additional property that derives from the fact that it represents a CPTP map:

$$\int_{\beta \in \mathbb{C}^M} d^{2M} \beta \Lambda_{\mathcal{E}}^{(s',s)}(\alpha, \beta) = 1. \quad (10)$$

In Section 3, we will use that (10) implies, whenever $\Lambda_{\mathcal{E}_i}^{(s',s)}$ is a regular and positive function, that we can interpret $\Lambda_{\mathcal{E}_i}^{(s',s)}(\alpha, \beta)$ as a probability distribution for β , for every possible value of α .

For a general multimode system eq. (9) is usually very hard to work out explicitly. This should not come as a surprise, given that, for setups with factorized multi-mode input states and single-mode measurements, the map \mathcal{E} should provide the necessary entanglement to make the setup hard to simulate on a classical computer. It is therefore common to make some assumptions on \mathcal{E} .

In [20], the authors focus on boson sampling and, thus, concentrate primarily on the case where \mathcal{E}_L is a passive linear optics channel. In this case, it is possible to find an analytical expression for $\Lambda_{\mathcal{E}_L}^{(s',s)}(\alpha, \beta)$ by using that $\mathcal{E}_L(\hat{D}^\dagger(\xi)) = \hat{D}^\dagger(L^\dagger \xi)$. Here L is an $M \times M$ matrix with $L^\dagger L \leq \mathbb{1}_M$ that captures, both, the mixing of the input modes and losses. This led to the key result that $\Lambda_{\mathcal{E}_L}^{(s',s)}(\alpha, \beta)$ is positive if and only if s and s' satisfy the following condition

$$\mathbb{1}_M - L^\dagger L - s + L^\dagger s' L \geq 0. \quad (11)$$

When it is possible to find s and s' such that condition (11) is satisfied, and such that $W_{\hat{\rho}_{in}}^{(s')}(\alpha)$ and $W_{\hat{\Pi}_x}^{(-s)}(\beta)$ are both positive and can therefore be treated as PDF, one can efficiently simulate the sampling process.

$$p(x) = \pi^M \int \dots \int W_{\hat{\rho}_{in}}^{(s_1)}(\alpha_1) \Lambda_{\mathcal{E}_1}^{(-s_1, s_2)}(\alpha_1, \alpha_2) \Lambda_{\mathcal{E}_2}^{(-s_2, s_3)}(\alpha_2, \alpha_3) \dots \dots \Lambda_{\mathcal{E}_k}^{(-s_k, s_{k+1})}(\alpha_k, \alpha_{k+1}) W_{\hat{\Pi}_x}^{(-s_{k+1})}(\alpha_{k+1}) d\alpha_1 \dots d\alpha_{k+1}. \quad (13)$$

Here, the factorized input state $\hat{\rho}_{in}$ of M modes can be represented by a factorized (s_1) -ordered quasi-PDF $W_{\hat{\rho}_{in}}^{(s_1)}(\alpha_1)$, and the measurement process is described by a quasi-PDF $W_{\hat{\Pi}_x}^{(-s_{k+1})}(\alpha_{k+1})$.

If there exists a set $\{s_i\}_{i \in [1, k+1]}$ so that each phase-space representation appearing in the decomposition (13) is regular and positive, the whole scheme can be classically simulated in an efficient way, using the same strategy as the one followed in [31], based on the fact that we can perform each step by sampling

Despite the interest of this result, the class of operations that can be described by such a \mathcal{E}_L is rather limited by the fact that it is a linear optical operation; on the other hand, when we aim at studying quantum advantage in CV systems, it is crucial to include a wider range of operations that can induce squeezing and non-Gaussianity.

In this work, we will also make an assumption on \mathcal{E} , namely that the total channel is decomposed in many operations: $\mathcal{E} = \mathcal{E}_1 \circ \mathcal{E}_2 \circ \dots \circ \mathcal{E}_k$. In the context of quantum computing, we typically understand this as a decomposition in quantum gates, i.e. other CPTP quantum channels involving at most $n \ll M$ modes each. In Section 4 we restrict to the common cases of single- and two-mode operations, but the results of Section 3 can be applied more generally. To study this sequence of operations, we rely on the composition rule

$$\Lambda_{\mathcal{E}_1 \circ \mathcal{E}_2}^{(s',s)}(\alpha, \beta) = \int_{\gamma \in \mathbb{C}^M} d^{2M} \gamma \Lambda_{\mathcal{E}_1}^{(s',s'')}(\alpha, \gamma) \Lambda_{\mathcal{E}_2}^{(-s'',s)}(\gamma, \beta). \quad (12)$$

The fact that an operation only acts on n modes is reflected by the fact that these functions involve at most n components of α, β , and γ each, and behave like delta distributions on the remaining $M-n$ modes.

3 Simulation of Sampling Algorithms

In fig. 2, we show a schematic representation of the full sampling protocol that is considered in our work: a factorised input state $\hat{\rho}_{in} = \hat{\rho}_1 \otimes \dots \otimes \hat{\rho}_M$ is sent through a CPTP channel $\mathcal{E} = \mathcal{E}_1 \circ \mathcal{E}_2 \circ \dots \circ \mathcal{E}_k$, and is ultimately measured by a set of single-mode detectors with POVM elements $\hat{\Pi}_x = \hat{\Pi}_{x_1} \otimes \dots \otimes \hat{\Pi}_{x_M}$. In phase-space, we can generalise eq. (8) to describe the probability to obtain a string of measurement outcomes $x = (x_1, \dots, x_M)$, associated with POVM element $\hat{\Pi}_x$, as

a probability distribution (see the second part of Algorithm 1). We thus seek to optimise on each s_i , which will eventually lead us to Algorithm 1 to check whether a scheme, that follows the general structure of fig. 2, can be efficiently simulated by classical means.

To explain this optimisation of s_i parameters, we start with the input state. By virtue of eq. (6), for any single-mode state $\hat{\rho}$ there exists a maximal value $\tau_{\hat{\rho}} \in [-1, +1]$ such that $W_{\hat{\rho}}^{(s)}$ is a probability den-

sity function for any $s \leq \tau_{\hat{\rho}}$. The positivity of the Husimi Q-representation on top guarantees that such a parameter $\tau_{\hat{\rho}}$ can always be found.

The study of the transfer functions $\Lambda_{\mathcal{E}_i}^{(-s_i, s_{i+1})}(\alpha_i, \alpha_{i+1})$ is somewhat more subtle. We note, first of all, that we can easily derive a result similar to eq. (4) for $s'_i \succ s_i$ and $s'_{i+1} \prec s_{i+1}$ (as matrix inequalities):

$$\begin{aligned} \Lambda_{\mathcal{E}_i}^{(-s'_i, s'_{i+1})}(\alpha_i, \alpha_{i+1}) &= \frac{2}{\det(s_{i+1} - s'_{i+1}) \det(s'_i - s_i)} \\ &\times \iint_{\beta, \gamma \in \mathbb{C}^M} \frac{d^{2M} \beta d^{2M} \gamma}{\pi^{4M}} e^{-2(\alpha_i - \beta)^\dagger (s'_i - s_i)^{-1} (\alpha_i - \beta)} \\ &\times e^{-2(\alpha_{i+1} - \gamma)^\dagger (s_{i+1} - s'_{i+1})^{-1} (\alpha_{i+1} - \gamma)} \\ &\times \Lambda_{\mathcal{E}_i}^{(-s_i, s_{i+1})}(\beta, \gamma). \quad (14) \end{aligned}$$

Since we are convoluting with a Gaussian, the function gets smoother and negative regions become shallower (see eq. (4)). Due to the sign difference, the same happens for $s'_{i+1} \prec s_{i+1}$. In other words, the phase-space representation $\Lambda_{\mathcal{E}_i}^{(-s_i, s_{i+1})}$ behaves more and more like a positive kernel as we increase s_i and decrease s_{i+1} .

At the i th step in the for-loop of Algorithm 1, the input ordering parameters τ_i are fixed in the previous step, $i - 1$, to be as high as possible. As implied by eq. (14), this also makes $\Lambda_{\mathcal{E}_i}^{(-\tau_i, s_{i+1})}$ as close to being regular and positive as possible, therefore we shall now focus just on the effect of the output parameters s_{i+1} to show the consistency of our algorithm.

This maximal value will then become τ_{i+1} . By virtue of eq. (14), the procedure of maximising s_{i+1} in step i of Algorithm 1 guarantees the best possible choice for the first ordering parameters in the transfer function of step $i + 1$. Nevertheless, at any stage of the for-loop, it is possible that no appropriate ordering parameter can be found to guarantee that the transfer function is a positive kernel. In that case, the algorithm fails, and we cannot simulate (13) through sampling in this manner, one would need to find another way to compile the gates, as it is discussed in the outlook.

If we do make it all the way to the final step, we find a fixed parameter τ_{k+1} for which we have to evaluate the POVM elements $W_{\hat{\Pi}_x}^{(-\tau_{k+1})}(\alpha_{k+1})$. The function $W_{\hat{\Pi}_x}^{(-\tau_{k+1})}$ is a product of single-mode functions $W_{\hat{\Pi}_x}^{(-\tau_{k+1}^{(j)})}$, with $\int_{x \in \mathcal{X}_j} dx \hat{\Pi}_x = \mathbb{1}$. The set \mathcal{X}_j denotes the set of all possible measurement outcomes for the detector that measures the j th mode. This implies that every local detector is described by a set of phase-space representations $\{W_{\hat{\Pi}_x}^{(-s)}(\alpha) \mid x \in \mathcal{X}_j\}$ that satisfy the condition

$$\pi \int_{x \in \mathcal{X}_j} dx W_{\hat{\Pi}_x}^{(-\tau_{k+1}^{(j)})}(\alpha) = 1, \quad (15)$$

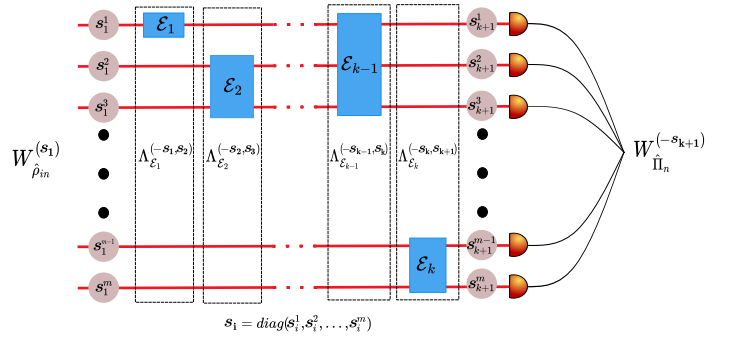


Figure 2: Generic quantum-optical scheme depicted by M input modes, described by a density operator ρ_{in} processed through a trace-preserving quantum channel \mathcal{E} , who can be decomposed into a sequence of trace-preserving quantum channels $\mathcal{E} = \mathcal{E}_1 \circ \mathcal{E}_2 \circ \dots \circ \mathcal{E}_k$. This produce the output state $\hat{\rho}_{out} = \mathcal{E}(\hat{\rho}_{in})$ and an output probability distribution $p(\mathbf{x}) = \text{Tr}[\hat{\rho}_{out} \hat{\Pi}_{\mathbf{x}}]$ sampled by measuring the POVM $\hat{\Pi}_{\mathbf{x}}$.

which must hold for all $\alpha \in \mathbb{C}$. For the simulation algorithm to work, we must be able to sample a final measurement outcome \mathbf{x} that describes the click in all the detectors. When the resulting parameter τ_{k+1} is such that the functions $W_{\hat{\Pi}_x}^{(-\tau_{k+1}^{(j)})}(\alpha)$ are positive functions for all possible measurement $x \in \mathcal{X}_j$, for all the modes j , we can treat the functions $\pi W_{\hat{\Pi}_x}^{(-\tau_{k+1}^{(j)})}(\alpha)$ as probability distributions on the space $x \in \mathcal{X}_j$. If this is the case, we can sample the measurement outcomes for all the individual detectors and finally obtain \mathbf{x} in a way that is consistent with probability density (13).

The previously described optimisation scheme for the ordering parameters explains the foundations of Algorithm 1. This algorithm effectively reduces the problem of the positivity of the quasiprobability distributions to a study of the ordering parameters, we are only concerned with those parameters and how they change during the computation. Indeed, Algorithm 1 fixes ordering parameters layer by layer, and we can understand this as an evolution of the initial ordering parameters (and thus nonclassical depth) of the input state throughout the different stages of the algorithm. Once the ordering parameters are fixed, the sampling algorithm is the same as the one proposed by Ref. [31]. Considerations on computational complexity of the sampling algorithm were already provided there.

We should emphasise some key assumptions from the computational point of view. First of all, we assume that the circuit decomposition $\mathcal{E} = \mathcal{E}_1 \circ \mathcal{E}_2 \circ \dots \circ \mathcal{E}_k$ is known. Furthermore, we assume that for all the elements in the circuit (input states, gates, and measurements) the (s) -parameterised phase space representations in (13) are known (or can be calculated at a negligible overhead). Finally, we assume that it is computationally efficient to sample from these PDFs

Algorithm 1: Classical simulation algorithm for a quantum computational scheme following the general structure of Figure (2). Notice that in the last step β_{k+1} is fixed and $\pi^M W_{\Pi_{\mathbf{x}}}^{(-\tau_{k+1})}(\beta_{k+1})$ is a PDF in \mathbf{x} .

input : set of functions
 $W_{\hat{\rho}_{in}}^{(s_1)}, \{\Lambda_{\mathcal{E}_k}^{(-s_i, s_{i+1})}\}_{i \in [1, k]}, W_{\Pi_{\mathbf{x}}}^{(-s_{k+1})}$

output: a sample of measurement outcomes according to $p(\hat{x})$ (result of classical simulation), failed (classical simulation not possible)

begin

▷ *First the optimization*

find the max s_1 s.t. $W_{\hat{\rho}_{in}}^{(s_1)}(\alpha_1)$ is non-negative ;

let $\tau_1 := \max(s_1)$;

for $i \in [1, k]$ **do**

find max s_{i+1} s.t. $\Lambda_{\mathcal{E}_i}^{(-\tau_i, s_{i+1})}(\alpha_i, \alpha_{i+1})$ is non-negative ;

if no such s_{i+1} can be found **then**

| return: failed ;

end

else

| let $\tau_{i+1} := \max(s_{i+1})$;

end

end

if $W_{\Pi_{\mathbf{x}}}^{(-\tau_{k+1})}(\alpha_{k+1})$ is non-negative for τ_{k+1} **then**

| proceed to sampling ;

end

else

| return: failed ;

end

▷ *Then the sampling*

sample a point α_1 according to $W_{\hat{\rho}_{in}}^{(\tau_1)}(\alpha_1)$;

$\beta_1 := \alpha_1$;

for $i \in [1, k]$ **do**

sample a point α_{i+1} according to $\Lambda_{\mathcal{E}_i}^{(-\tau_i, \tau_{i+1})}(\beta_i, \alpha_{i+1})$;

$\beta_{i+1} := \alpha_{i+1}$;

end

sample a string of outcomes \mathbf{x} according to $\pi^M W_{\Pi_{\mathbf{x}}}^{(-\tau_{k+1})}(\beta_{k+1})$;

return: \mathbf{x} ;

end

once they are positive. This final assumption may break down once the functions oscillate too rapidly, an effect which is in principle captured by the stellar rank [37].

To encapsulates, in broad terms, the fundamental principle underlying the present method we propose the following simplified thought experiment. Let us assume that a single-mode highly non-classical state goes through a specific channel whose transfer function, $\Lambda_{\mathcal{E}}^{(-\tau_{in}, \tau_{out})}$, is positive only for τ_{out} arbitrarily close to 1. The inherent characteristic of the input state would force the first parameter to assume a value τ_{in} close to -1 . Indeed, if one wishes to erase all negativity from the Wigner function of such a state, one would have to proceed all the way to the smooth, completely positive Husimi Q -function by convolving said Wigner function with a broad Gaussian. As such, the channel has effectively transformed an input state that is highly non-classical into an output state that is highly classical; a greater range of quasi-PDF behave as PDF at the output than at the input. Such a channel would represent a point in the computation where all potential quantum advantage that might have been provided by the nonclassical input is effectively lost. This channel is ineffective in terms of providing a quantum advantage, as it effectively negates the potential benefits of imputing a Wigner negative state. This highlights that it is crucial to understand the relation between the parameters τ_i and τ_{i+1} that are selected by Algorithm 1. Therefore, in the next section, we will examine different elementary gates and observe how the ordering parameter evolves through them.

4 Resourcefulness of Gates

4.1 Conditions for a general unitary

Before delving into less trivial examples, important conclusions on the ordering parameters can be drawn by studying the identity channel. Since it acts independently on each mode, we will detail it for a single mode. Moreover, given that this channel leaves any input state unchanged, it cannot modify the nonclassical depths. Consider then an input state $\hat{\rho}$ such that $W_{\hat{\rho}}^{(s_i)}$ is a regular probability density function and s_i is the largest possible value, i.e. corresponding to the nonclassical depth. If the transition kernel $\Lambda_{\mathbf{1}}^{(-s_i, s_{i+1})}$ were to be positive and regular for $s_{i+1} > s_i$, we would obtain as an output a function $W_{\hat{\rho}}^{(s_{i+1})}$ which is still regular and positive, contradicting the hypothesis that s_i was the largest value. This implies that a necessary condition for $\Lambda_{\mathbf{1}}^{(-s_i, s_{i+1})}$ to be regular and positive is that $s_{i+1} \leq s_i$, which is also a sufficient condition by eq. (11) with $L = \mathbf{1}$ being the identity matrix. When this condition is met $\Lambda_{\mathbf{1}}^{(-s_i, s_{i+1})}$ is a Gaussian function in its input and output variables,

while for $s_{i+1} > s_i$ it is a singular distribution attaining divergent values almost everywhere.

By the same token, it can be foreseen that for a single-mode unitary channel \hat{U} the condition $s_{i+1} \leq s_i$ is still necessary in order for $\Lambda_{\hat{U}}^{(-s_i, s_{i+1})}$ to be regular and positive, otherwise \hat{U} could increase the nonclassical depth of *any* input state with initial nonclassical depth t . Let us prove this formally by considering how the equality $\hat{U}\hat{U}^\dagger = \mathbb{1}$ rewrites in terms of s -ordered quasi-PDF:

$$\int_{\alpha_2 \in \mathbb{C}} d^2\alpha_2 \Lambda_{\hat{U}}^{(-s_i, s_{i+1})}(\alpha_1, \alpha_2) \Lambda_{\hat{U}^\dagger}^{(-s_{i+1}, s_{i+1})}(\alpha_2, \alpha_3) = \Lambda_{\mathbb{1}}^{(-s_i, s_{i+1})}(\alpha_1, \alpha_3). \quad (16)$$

Formally, we can write the right-hand side as:

$$\Lambda_{\mathbb{1}}^{(-s_i, s_{i+1})}(\alpha_1, \alpha_3) = \int_{\xi \in \mathbb{C}} d^2\xi e^{(\alpha_1 - \alpha_3)\xi^\dagger - (\alpha_1 - \alpha_3)^\dagger \xi} \times e^{\xi(s_{i+1} - s_i)\xi^\dagger / 2}. \quad (17)$$

If $s_{i+1} > s_i$, the former expression diverges almost everywhere in α_1, α_3 , whereas for $s_{i+1} = s_i$ it reduces to the delta distribution, imposing $\alpha_1 = \alpha_3$. Now if $\Lambda_{\hat{U}}^{(-s_i, s_{i+1})}$ were to be a regular, positive semidefinite function¹, the result of the left-hand side in eq. (16) cannot be divergent, even if $\Lambda_{\hat{U}^\dagger}^{(-s_{i+1}, s_{i+1})}$ is a very singular distribution, which implies that indeed $\Lambda_{\hat{U}}^{(-s_i, s_{i+1})}$ can never be a regular probability density function if $s_{i+1} > s_i$. Notice that when $s_{i+1} = s_i$ we could have, in the best case, that $\Lambda_{\hat{U}}^{(-s_i, s_{i+1})}$ is as singular as a delta distribution and then eq. (16) still holds even if the right-hand side diverges for $\alpha_1 = \alpha_3$.

4.2 Losses

Before providing the characterization of a universal set of unitary quantum gates, it is instructive to contrast the general result that we got for unitary channels with the prototypical example of dissipative quantum channels, i.e. losses which are crucial in modelling optical setups and deserves an additional discussion in its own right. The optical loss channel is implicitly already covered in Ref. [20] where eq. (11) is derived to describe a linear optics network with losses. To consider optical losses in the spirit of our gate-based protocol of fig. 2, we can just define a single-mode loss channel $\Lambda_{\mathcal{E}_\eta}^{(-s_i, s_{i+1})}(\alpha, \beta)$ as a single-mode version of eq. (11) setting $L = \sqrt{\eta}$, where $\eta \in [0, 1]$ describes the efficiency of the channel ($\eta = 1$ reflects the absence of losses, while $\eta = 0$ means that

¹We shall assume that whenever an s -ordered quasiprobability is regular and non-negative, it also belongs to the Schwartz space of rapidly decreasing function, so that no issues of convergence can arise with respect to tempered distributions. This is typically the case, since this probability density functions decay as Gaussians for large absolute values of their arguments.

the state is completely lost). We can from this find a decreasing linear relation with respect to s_i :

$$s_{i+1} \geq 1 - \eta(1 - s_i). \quad (18)$$

Since $s_i = (1 - \eta)s_i + \eta s_i < 1 - \eta(1 - s_i)$, this implies that we can always pick $s_{i+1} > s_i$ for $\eta < 1$ and, the smaller the value of η , the closest the maximum value of s_{i+1} approaches 1, as shown in fig. 1. It can thus be concluded that losses always result in a more classical output, in stark contrast with the opposite result that we derived for unitary gates 16, thereby emphasizing the peculiar nature of losses for nonclassicality. This relatively straightforward result, moreover, allows us to understand how losses can hinder a possible quantum computational advantage. In a real circuit, loss channels of the type $\Lambda_{\mathcal{E}_\eta}^{(s_i, s_{i+1})}$ can occur everywhere, effectively increasing the chances of success of Algorithm 1 at any step. As is commonly done in quantum optics, we can now describe realistic operations and measurements by taking ideal unitary ones and adding a loss channel at the input and output. When we add them in between the gates and run Algorithm 1, we can now deal with mode-dependent losses, which are often overlooked in studies of sampling problems.

Finally, it is worth mentioning that losses allow us to consider in principle values of the s parameters outside the range $[-1, 1]$: indeed a coherent state going through a loss channel will become a displaced thermal state, whose s -ordered quasi-PDF will be a regular and positive function also for some values of $s > 1$, defined again through Eq.(1). In general, problems might arise because the s -ordered quasi-PDFs of channels and states for values of $s > 1$ are not guaranteed to exist, even in the sense of distributions, and they are not associated with an ordering of the creation and annihilation operators. However, if we have input states that are mixed and noisy, such that they *can* be parametrized with values of s larger than 1, the matching rule in Eq. (3) ensures that at the next step we will have an even more regular function (since s matches with $-s$) and we can possibly have more chances to find a positive decomposition of the whole circuit by going beyond the limitation of $s \in [-1, 1]$.

5 Characterization of a Universal Set of Unitary Gates

Algorithm 1 is based on the idea that we have at hand a decomposition of the full photonic quantum circuit into a set of previously characterized gates, such that the computational effort needed to compute the (s)-ordered quasi-PDFs for such elements constitutes just a fixed preliminary overhead with respect to the actual simulation cost of the computation through sampling. It is thus consequential to characterize a universal set of unitary gates, with which all CV unitary operations can be approximated efficiently [42]; one

such set is provided by *two-mode Gaussian unitary gates* and one single-mode non-Gaussian gate, such as *the cubic phase gate* [43], whose characterizations are provided in the following.

5.1 Gaussian unitaries

Among Gaussian unitary gates, displacements and single-mode phase shifters clearly do not affect the nonclassicality (hence they leave the value of the s -parameters unchanged), since they act as Euclidean transformations on quasi-PDFs. Thus, we only need to consider squeezers and beam splitters. We will show that the action of a squeezing gate can directly alter the s parameter of the output, whereas beam splitters can “mix” the s parameters of their input modes.

5.1.1 Squeezing gate

Starting with the squeezing gate, denoted by \mathcal{S} , the trace-preserving quantum gate \mathcal{S} acting on the displacement operator is:

$$\mathcal{S}(\hat{D}^\dagger(\xi)) = \hat{S}^\dagger(r)D^\dagger(\xi)\hat{S}(r) = \hat{D}^\dagger(\chi), \quad (19)$$

where $\hat{S}(r)$ is the squeezing operator for a squeezing parameter r and $\chi = \xi \cosh r + \xi^\dagger \sinh r$. Thus implementing a simple re-scaling of the displacement operator. For \mathcal{S} the transfer function take the form

$$\begin{aligned} \Lambda_{\mathcal{S}}^{(s_i, s_{i+1})}(\alpha, \beta) &= \iint \frac{d^2\zeta}{\pi^2} \frac{d^2\xi}{\pi} e^{\beta\zeta^\dagger - \zeta\beta^\dagger} e^{\zeta s_{i+1}\zeta^\dagger/2} e^{\xi\alpha^\dagger - \alpha\xi^\dagger} e^{\xi s_i \xi^\dagger/2} \\ &\quad \times Tr[\mathcal{S}(\hat{D}^\dagger(\xi))\hat{D}(\zeta)]. \end{aligned} \quad (20)$$

We can write

$$\mathcal{S}(\hat{D}^\dagger(\xi)) = e^{\chi\chi^\dagger} \int \frac{d^2\gamma}{\pi} e^{\gamma\xi^\dagger - \xi\gamma^\dagger} |\gamma\rangle \langle \gamma|. \quad (21)$$

And we can use the normally ordered form of the displacement operator, $\hat{D}(\zeta) = e^{-\zeta\zeta^\dagger/2} e^{\zeta\hat{a}^\dagger} e^{-\hat{a}\zeta^\dagger}$ to obtain

$$Tr[\mathcal{S}(\hat{D}^\dagger(\xi))\hat{D}(\zeta)] = \pi e^{\chi\chi^\dagger/2} e^{\zeta\zeta^\dagger/2} \delta(\zeta - \chi) \quad (22)$$

Thus the transfer function (20) becomes

$$\Lambda_{\mathcal{S}}^{(-s_i, s_{i+1})}(\alpha, \beta) = \int d\xi e^{\chi^\dagger\beta - \chi\beta^\dagger + \frac{\chi s_{i+1}\chi^\dagger}{2}} e^{\xi^\dagger\alpha - \xi\alpha^\dagger + \frac{\xi s_i \xi^\dagger}{2}} \quad (23)$$

As one can notice from this form the transfer function is well behave and non-negative if and only if

$$\sigma^{-1} = \begin{aligned} &[(\xi \cosh r + \xi^\dagger \sinh r)s_{i+1}(\xi^\dagger \cosh r + \xi \sinh r) \\ &-s_i|\xi|^2]^{-1} \geq 0 \end{aligned} \quad (24)$$

Finally, we find that one can sample from the transfer function, and thus classically simulate this block if

and only if

$$\begin{cases} s_{i+1} \leq \frac{s_i}{e^{2|r|}} & \text{if } s_i \geq 0 \\ s_{i+1} \leq \frac{s_i}{e^{-2|r|}} & \text{if } s_i \leq 0 \end{cases} \quad (25)$$

Therefore, in general, the squeezing channel requires us to parametrize the output expecting it to have a greater nonclassical depth (lower maximum value allowed for s) in order for the transfer function to be a positive transfer probability kernel. It is interesting to note that the conditions linearly bound one ordering parameter with respect to the other and they are fully symmetric under the exchange $-s_i \leftrightarrow s_{i+1}$, as can be seen more clearly from Fig. (3(a)), where we plot in gray the region in the (s_i, s_{i+1}) plane where $\Lambda_{\mathcal{S}}^{(-s_i, s_{i+1})}$ is non-negative, for $r = 0.3$.

Notice that, for $s_i < 0$, the upper bound $s_i/e^{-2|r|}$ can be smaller than -1 , namely if $|r| > -\frac{1}{2} \ln |s_i|$, therefore for sufficiently nonclassical, Wigner negative input states the squeezing channel cannot be simulated through Algorithm 1, no matter how the output is parametrized. This observation provides a first hint of the fact that non-Gaussian resources are pivotal for possible quantum advantages.

It is crucial to stress that one could include the squeezing channel into the previous channel that was applied to the multi-mode system and try to simulate it as a single block with a positive transfer probability kernel, possibly finding less strict conditions for the output parameter s_{i+1} ; however, when the previous channel is multi-mode and potentially entangling, this forces us to apply the squeezing to a multi-mode state, converting the challenge of simulating the possibly negative squeezing transfer function into that of simulating a positive transfer function on a larger space.

A special point deserves now our attention, the output state of the squeezing channel may not be more non-classical than the input. It is evident that the conditions set out in eq. (25) pertain to the positivity and well-behavedness of the transfer function. In the event that the aforementioned conditions are not met, the transfer function will exhibit negative region(s) and/or will be highly singular, thereby implying that one cannot sample from it efficiently [44]. Nevertheless, it is possible for the output state to be, in all respects and according to all characterisations, classical. This can be understood by imagining a highly squeezed input state going through a squeezing channel with the opposite squeezing parameter and resulting in a more classical output. Through the action of \mathcal{S} , we then squeeze in the orthogonal direction, by the same factor of r . In this case, the output state would be very classical. However, if the conditions set out in (25) are not met, it is not possible to sample from the transfer function describing the process.

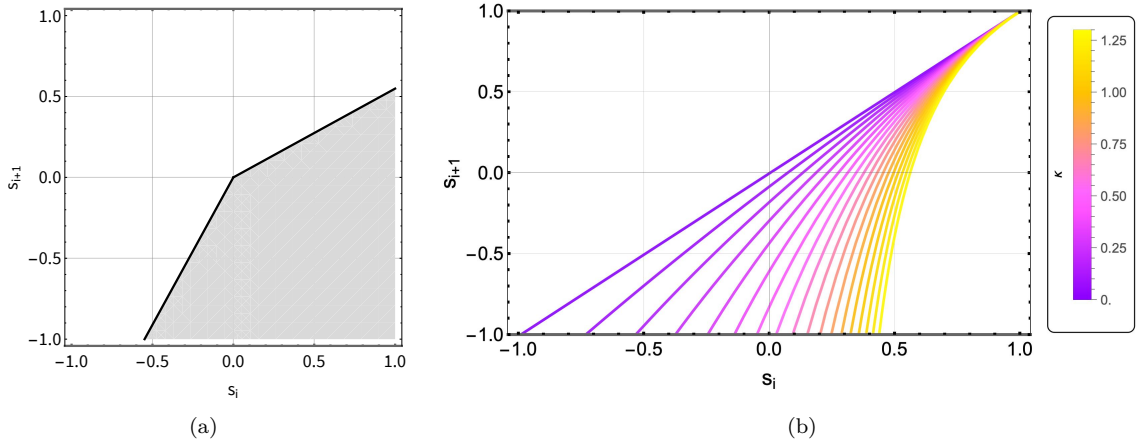


Figure 3: (a) On the squeezing gate: the region in the (s_i, s_{i+1}) plane where $\Lambda_S^{(-s_i, s_{i+1})}$ is non-negative according to eq. (25) is displayed in gray, for $r = 0.3$. (b) On the single-photon subtraction: limit lines according to eq. (30) for various values of $\alpha \in [0, 1]$, represented by different shadings. For each value of α , the allowed values of s_{i+1} to have a non-negative transfer functions of the BS lie under the respective curve.

5.1.2 Beam-splitter

We shall now proceed to identify the conditions under which the beam-splitter (BS) can be considered a resourceful gate. Assume that we encounter a BS gate on block i , where $1 < i \leq k$. In a formal sense, our objective is to construct a channel \mathcal{E}^{BS} that acts as a beam-splitter transformation between two modes and trivially on the remaining $M - 2$ modes. Denoting by a and b the two modes on which the BS acts non-trivially, according to eq. (11) the limiting condition relating output to input ordering parameters is obtained by taking L is a unitary matrix describing the beam-splitter transformation,

$$L = \begin{pmatrix} \cos \theta & \sin \theta \\ -\sin \theta & \cos \theta \end{pmatrix}, \quad (26)$$

and $\theta \in \mathbb{R}$. Potential phase factors $e^{i\phi}$, representing the phase shift between the input modes of the beam splitter, has not been taken into account since the phase shift channel has no impact on the ordering parameter, merely rotating phase-space distributions without altering their values. By virtue of unitarity, the equation ultimately simplifies to:

$$\min \text{eig} \left(-\text{diag}(s_{i+1}^a, s_{i+1}^b) + L^\dagger \text{diag}(s_i^a, s_i^b) L \right) = 0. \quad (27)$$

While the relation between the input and output parameters is not very insightful at first glance, we do see that s_{i+1}^a will generally depend on both s_i^a and s_i^b (and analogously for s_{i+1}^b).

5.2 Realistic protocol for single-photon subtraction

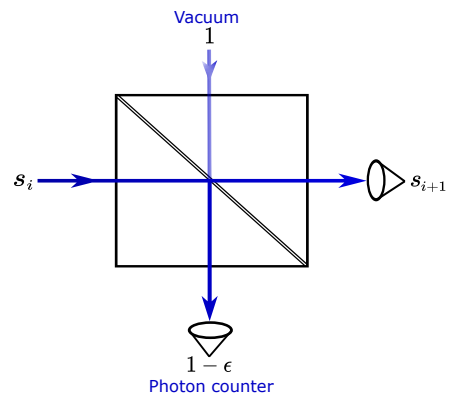


Figure 4: Realistic single-photon subtraction protocol seen from the perspective of our framework, where we consider solely the order parameter of the states on each branch.

In order to showcase the usefulness of the proposed protocol, we will apply it to the single-photon subtraction operation which is commonly considered as one of the most accessible de-Gaussifying procedures. We model realistic single-photon subtraction with a BS whose input modes are respectively the input state on which we wish to subtract a photon on one branch, and the vacuum state on the other. The transmittance $\eta = \cos^2 \theta$ of the BS with respect to the first mode is close to 1, meaning that only a small fraction of the signal will be reflected. On this weak output signal, a photon counter with some finite efficiency will be implemented, corresponding to the ideal POVM ($\epsilon = 0$) with elements $\{\hat{\Pi}_1 = |1\rangle\langle 1|, \hat{\Pi}_0 = \mathbb{1} - |1\rangle\langle 1|\}$. At the last step, only the outcomes corresponding to $\hat{\Pi}_1$ are post-selected. This measurement will be modelled choosing an ordering parameter close

to -1 , since the only value such that the s -ordered quasi-PDF of $|1\rangle\langle 1|$ is positive is -1 , being a projector on a highly non-classical state, but we shall assume that its value is $-1 + \epsilon$ to account for imperfect measurements. This proposed model is illustrated in fig. 4.

This results in the following set of input-output ordering parameters:

$$\mathbf{s}_{in} = \begin{pmatrix} s_i & 0 \\ 0 & 1 \end{pmatrix}; \quad \mathbf{s}_{out} = \begin{pmatrix} s_{i+1} & 0 \\ 0 & 1 - \epsilon \end{pmatrix} \quad (28)$$

recalling that the output parameter for the mode that

$$\lambda_{min} = \frac{1}{2} \left[s_i - s_{i+1} - \sqrt{(1 - s_i)^2 + (1 - s_{i+1})^2 - 2(1 - s_i)(1 - s_{i+1}) \cos 2\theta} \right] \geq 0. \quad (29)$$

For $-1 \leq s_{i+1} \leq s_i \leq 1$, this quantity is zero if θ is a multiple of π , including $\theta = 0$, and it is negative otherwise. Therefore we conclude that there exists no set of input-output parameters such that the transfer function is well-behaved in the case of perfect photodetection. This result is of great importance as it demonstrates that ideal single-photon detectors are sufficient to render this building-block impossible to simulate classically.

There exists however a nontrivial limit, tuning in on the scaling $\theta \propto \sqrt{\epsilon}$. In this case, taking the limit $\epsilon \rightarrow 0$ with $\theta = \kappa\sqrt{\epsilon}$ for a free tuning parameter $\kappa \in \mathbb{R}$, we can rewrite the condition $\lambda_{min} \geq 0$ as:

$$s_{i+1} \leq \frac{s_i - (1 - s_i)\kappa^2}{1 - (1 - s_i)\kappa^2}. \quad (30)$$

In fig. 3(b) these curves for various values of κ are displayed, with smaller values corresponding to shades towards the violet. We notice that, for each value of $\kappa > 0$, there is a minimum s_i under which no solution exist (each curve reaches the value $s_{i+1} = -1$ for some s_i strictly greater than -1). Furthermore, for $\kappa > \frac{1}{2}$ this limiting value for s_i is strictly positive, meaning that the single-photon subtraction modelled by this limit cannot be described with a non-negative transfer function whenever we input a Wigner-negative state. Significantly though, this implies that if we input noisy squeezed states, at fixed detection efficiency and transmittance, there is a maximum ratio of squeezing over noise after which the transfer function will never be positive, rendering this block non-simulatable even if the input is Wigner-positive.

Finally, let us note that the above arguments are purely based on the order parameters and do not require any further details of the phase-space representations. This means that this reasoning can be trans-

is measured has the opposite sign with respect to the ordering parameter that we had to choose for the highly nonclassical measurement. The resulting output parameter, s_{i+1} , with which we have to parameterize the output to have a positive transfer function for the beam-splitter will depend on the only free parameter: the ordering parameter of the input state. Clearly, if we take the limit $\theta \rightarrow 0$ for finite ϵ the result will be trivial, having $s_{i+1} \leq s_i$ as the only condition. Going back to eq. (27), inserting the diagonal matrices above and imposing that the smallest eigenvalue is non-negative, for an ideal detection ($\epsilon = 0$) with generic mixing angle θ we find instead:

posed to essentially all other measurement-based operations.

5.3 The cubic phase gate

Having seen that only Wigner negative inputs can force the squeezing channel to be represented only by a negative transfer function, we will now tackle an instance of a non-Gaussian single-mode unitary channel of utmost relevance in the theory of CV quantum computation: the cubic phase gate. It can be described by the unitary operator $\hat{U}_\gamma = e^{-i\frac{\gamma}{3!}\hat{q}^3}$, where $\gamma \in \mathbb{R}$ is known as the *cubicity*. It is well known [42, 45, 46] that, together with Gaussian gates, the cubic gate is sufficient to attain universality with CV quantum computation.

As shown in Appendix (B), if we input a state whose nonclassical depth corresponds to τ into a cubic channel with transfer function $\Lambda_{\hat{U}_\gamma}^{(-\tau, s_{out})}$, this function will never be a PDF if either $-\tau$ or s_{out} (or both) are positive, in particular if the input state was Wigner negative. If τ is instead positive (corresponding to a Wigner-positive input state), the minimum of $\Lambda_{\hat{U}_\gamma}^{(-\tau, s_{out})}$ can be bounded from below by $-\epsilon$, for any $0 < \epsilon \ll 1$ by imposing a condition on s_{out} as a function of τ, γ and ϵ given by:

$$s_{out} < \tau - f(\epsilon)\gamma^{1/3} \quad (31)$$

where $f(\epsilon)$ is some function of the bound on negativity. Therefore, if $f(\epsilon)\gamma^{1/3} > 1$, there are values of $0 \leq \tau < f(\epsilon)\gamma^{1/3} - 1$ for which $\Lambda_{\hat{U}_\gamma}^{(-\tau, s_{out})}$ will necessarily attain values lower than $-\epsilon$.

6 Conclusions

6.1 Simulability of photonic circuits

Using the language of (s)-ordered quasiprobability distributions on optical phase-space, we detailed a

procedure to systematically assess the possibility of framing a computational photonic quantum process in terms of probability distributions updated through positive-semidefinite transition kernels. Whenever such a decomposition is possible, the process can be simulated efficiently by a classical algorithm, namely by sampling the starting probability distribution and applying the steps of the algorithm in order to compute the output. In doing so, we unveil further resources needed to ensure a possible quantum advantage, beyond the already established necessity of Wigner negativity. In particular, our method is able to determine which amount of losses is tolerable at each step in the quantum computation before making the corresponding process efficiently simulatable. We emphasize that the strength of our method heavily relies on the fact that the conditions for positivity of each transfer function are determined just by the ordering parameters, and therefore only by the nonclassical depth of the input and not on the specific quantum state. This property allows us to explicitly derive these positivity conditions for all Gaussian unitary channels. In particular, a single-mode squeezing channel can always be implemented by a positive transfer function by some choice of the second ordering parameter, unless the input is Wigner negative. Studying how a beam splitter mixes the nonclassicalities of the input and fixing a maximally nonclassical measurement, we deduce that (realistic) single-photon subtraction is not efficiently simulatable if the squeezing of the input is sufficiently high. Finally, we tackle the harder computation of the (s_1, s_2) -ordered function of the cubic gate to showcase the power of our method to provide quantitative answers also for non-trivial non-Gaussian gates and we determine in which regimes even the cubic gate is insufficient to achieve any quantum advantage.

6.2 Loss tolerance of photonic quantum gates and their resourcefulness

The presented techniques and results can not only directly be applied to existing photonic quantum circuits to test their simulability beyond the requirement of Wigner negativity, but they also probe the robustness of different circuit designs to losses. They allow us to pinpoint the most sensitive gates in the circuit and provide constraints for the quality of technological components that implement them. For example, taking figs. 3(a) and 3(b) for the squeezing and beam-splitter channels, respectively, we can interpret the minimal value of s_i attained by each curve (for $s_{i+1} = -1$) as quantifying the maximum amount of losses above which said gate can always be represented by a regular PDF, no matter the input state.

6.3 Outlook

Our results provide a significant step forward towards the goal of singling out the salient quantum features needed to hinder any attempt of simulating a photonic quantum process. Many directions remain to be explored, including but not limited to: the role of entanglement at preventing larger combinations of quantum gates, acting on fewer modes each, to be simulated in a single shot; the implications of the conditions on (s) -ordered quasiprobability distributions on the existence of local hidden variable models; the relation between common measures of Wigner negativity and the nonclassical depth of Wigner negative states, to determine which one best captures the quantitative aspects of this resource.

It is also interesting to explore what happens when we drop some of the computational assumptions. A first key step is to connect our approach to the problem of compiling. In the present work, we have assumed that the decomposition of the system in a sequence of fundamental gates is known. However, there may be many different decompositions that lead to the same global operation, leading to many possible routes for numerically simulating the sampling setup.

One may also argue that the computational cost of sampling from a probability distribution is not really taken into account. While from a probability theory point of view this is more a classical than a quantum problem, it is clear that quantum properties of states, gates, and measurements, may lead to highly oscillating PDFs on phase space. This features may render our simulation protocol extremely costly, even when Algorithm 1 would technically succeed. Moreover, the sampling cost has been explored through the lens of (s) -ordered quasiprobabilities in [47]. Given sufficient classicality, the output parameter can be made arbitrarily close to one for a single step. This suggests that the step in question may be simulatable in polynomial time. Furthermore, allowing for additive errors in the sampling allows for more space in the ordering parameter's optimisation algorithm.

Finally, one may want to challenge all together the idea that one cannot sample of the phase space representation manifests negativity. Indeed, it has been shown that we can use sampling techniques to deal with non-positive quasi-probabilities by paying an additional sampling cost [44] that is proportional to the negativity volume. Some recent work on the role of phase space negativity on quantum kernel methods [48] may help us get a more nuanced idea of the role of the negativity volume in cases where our Algorithm 1 fails.

Acknowledgments

We would like to thank our fellow theoreticians Carlos Lopetegui and Mathieu Isoard for the numer-

ous informative and supportive discussions. We thank Ulysse Chabaud for valuable comments on the manuscript. We acknowledge financial support from the ANR JCJC project NoRdiC (ANR-21-CE47-0005), the Plan France 2030 through the project OQuLus (ANR-22-PETQ-0013), and the HORIZON-EIC-2022- PATHFINDERCHALLENGES-01 programme under Grant Agreement Number 101114899 (Veriqub).

References

- [1] Peter W. Shor. “Polynomial-time algorithms for prime factorization and discrete logarithms on a quantum computer”. *SIAM Review* **41**, 303–332 (1999).
- [2] John M. Martyn, Zane M. Rossi, Andrew K. Tan, and Isaac L. Chuang. “Grand unification of quantum algorithms”. *PRX Quantum* **2**, 040203 (2021).
- [3] Scott Aaronson and Alex Arkhipov. “The computational complexity of linear optics”. In Proceedings of the Forty-Third Annual ACM Symposium on Theory of Computing. Page 333–342. STOC ’11 New York, NY, USA (2011). Association for Computing Machinery.
- [4] Michael J. Bremner, Richard Jozsa, and Dan J. Shepherd. “Classical simulation of commuting quantum computations implies collapse of the polynomial hierarchy”. *Proceedings of the Royal Society A: Mathematical, Physical and Engineering Sciences* **467**, 459–472 (2011).
- [5] Sergio Boixo, Sergei V. Isakov, Vadim N. Smelyanskiy, Ryan Babbush, Nan Ding, Zhang Jiang, Michael J. Bremner, John M. Martinis, and Hartmut Neven. “Characterizing quantum supremacy in near-term devices”. *Nature Physics* **14**, 595–600 (2018).
- [6] Aram W Harrow and Ashley Montanaro. “Quantum computational supremacy”. *Nature* **549**, 203–209 (2017).
- [7] Dominik Hangleiter and Jens Eisert. “Computational advantage of quantum random sampling”. *Rev. Mod. Phys.* **95**, 035001 (2023).
- [8] Frank Arute, Kunal Arya, Ryan Babbush, Dave Bacon, Joseph C. Bardin, Rami Barends, et al. “Quantum supremacy using a programmable superconducting processor”. *Nature* **574**, 505–510 (2019).
- [9] Han-Sen Zhong, Hui Wang, Yu-Hao Deng, Ming-Cheng Chen, Li-Chao Peng, Yi-Han Luo, Jian Qin, et al. “Quantum computational advantage using photons”. *Science* **370**, 1460–1463 (2020).
- [10] Lars S. Madsen, Fabian Laudenbach, Mohsen Falamarzi. Askarani, Fabien Rortais, Trevor Vincent, Jacob F. F. Bulmer, Filippo M. Miatto, Leonhard Neuhaus, Helt, et al. “Quantum computational advantage with a programmable photonic processor”. *Nature* **606**, 75–81 (2022).
- [11] Matthew DeCross, Reza Haghshenas, Minzhao Liu, Enrico Rinaldi, Johnnie Gray, Yuri Alexeev, Charles H. Baldwin, John P. Bartolotta, Matthew Bohn, et al. “The computational power of random quantum circuits in arbitrary geometries” (2024). [arXiv:2406.02501](https://arxiv.org/abs/2406.02501).
- [12] Craig S. Hamilton, Regina Kruse, Linda Sansoni, Sonja Barkhofen, Christine Silberhorn, and Igor Jex. “Gaussian boson sampling”. *Phys. Rev. Lett.* **119**, 170501 (2017).
- [13] A. P. Lund, A. Laing, S. Rahimi-Keshari, T. Rudolph, J. L. O’Brien, and T. C. Ralph. “Boson sampling from a gaussian state”. *Phys. Rev. Lett.* **113**, 100502 (2014).
- [14] U. Chabaud, T. Douce, D. Markham, P. van Loock, E. Kashefi, and G. Ferrini. “Continuous-variable sampling from photon-added or photon-subtracted squeezed states”. *Phys. Rev. A* **96**, 062307 (2017).
- [15] L. Chakhmakhchyan and N. J. Cerf. “Boson sampling with gaussian measurements”. *Phys. Rev. A* **96**, 032326 (2017).
- [16] Nicolás Quesada, Juan Miguel Arrazola, and Nathan Killoran. “Gaussian boson sampling using threshold detectors”. *Physical Review A* **98**, 062322 (2018).
- [17] Raúl García-Patrón, Jelmer J Renema, and Valery Shchesnovich. “Simulating boson sampling in lossy architectures”. *Quantum* **3**, 169 (2019).
- [18] Jelmer J Renema. “Simulability of partially distinguishable superposition and gaussian boson sampling”. *Physical Review A* **101**, 063840 (2020).
- [19] J. J. Renema, A. Menssen, W. R. Clements, G. Triginer, W. S. Kolthammer, and I. A. Walmsley. “Efficient classical algorithm for boson sampling with partially distinguishable photons”. *Phys. Rev. Lett.* **120**, 220502 (2018).
- [20] Saleh Rahimi-Keshari, Timothy C Ralph, and Carlton M Caves. “Sufficient conditions for efficient classical simulation of quantum optics”. *Physical Review X* **6**, 021039 (2016).
- [21] Jacob F. F. Bulmer, Bryn A. Bell, Rachel S. Chadwick, Alex E. Jones, Diana Moise, Alessandro Rigazzi, Jan Thorbecke, Utz-Uwe Haus, Thomas Van Vaerenbergh, Raj B. Patel, Ian A. Walmsley, and Anthony Laing. “The boundary for quantum advantage in gaussian boson sampling”. *Science Advances* **8**, eabl9236 (2022).
- [22] Haoyu Qi, Daniel J. Brod, Nicolás Quesada, and Raúl García-Patrón. “Regimes of classical simulability for noisy gaussian boson sampling”. *Phys. Rev. Lett.* **124**, 100502 (2020).
- [23] Nicolás Quesada, Rachel S. Chadwick, Bryn A. Bell, Juan Miguel Arrazola, Trevor Vincent,

- Haoyu Qi, and Raúl García–Patrón. “Quadratic speed-up for simulating gaussian boson sampling”. *PRX Quantum* **3**, 010306 (2022).
- [24] Peter D. Drummond, Bogdan Opanchuk, A. Delios, and M. D. Reid. “Simulating complex networks in phase space: Gaussian boson sampling”. *Phys. Rev. A* **105**, 012427 (2022).
- [25] Changhun Oh, Minzhao Liu, Yuri Alexeev, Bill Fefferman, and Liang Jiang. “Classical algorithm for simulating experimental gaussian boson sampling”. *Nature Physics* (2024).
- [26] Daniel Gottesman. “The heisenberg representation of quantum computers” (1998). [arXiv:quant-ph/9807006](https://arxiv.org/abs/quant-ph/9807006).
- [27] Stephen D. Bartlett, Barry C. Sanders, Samuel L. Braunstein, and Kae Nemoto. “Efficient classical simulation of continuous variable quantum information processes”. *Physical Review Letters* **88**, 097904 (2002).
- [28] Robin L Hudson. “When is the Wigner quasiprobability density non-negative?”. *Reports on Mathematical Physics* **6**, 249–252 (1974).
- [29] Francisco Soto and Pierre Claverie. “When is the Wigner function of multidimensional systems nonnegative?”. *Journal of Mathematical Physics* **24**, 97–100 (1983).
- [30] Kevin E Cahill and Roy J Glauber. “Density operators and quasiprobability distributions”. *Physical Review* **177**, 1882 (1969).
- [31] Andrea Mari and Jens Eisert. “Positive wigner functions render classical simulation of quantum computation efficient”. *Physical review letters* **109**, 230503 (2012).
- [32] Victor Veitch, Christopher Ferrie, David Gross, and Joseph Emerson. “Negative quasi-probability as a resource for quantum computation”. *New Journal of Physics* **14**, 113011 (2012).
- [33] Laura García-Álvarez, Cameron Calcluth, Alessandro Ferraro, and Giulia Ferrini. “Efficient simulatability of continuous-variable circuits with large Wigner negativity”. *Physical Review Research* **2**, 043322 (2020).
- [34] Cameron Calcluth, Alessandro Ferraro, and Giulia Ferrini. “Efficient simulation of Gottesman-Kitaev-Preskill states with Gaussian circuits”. *Quantum* **6**, 867 (2022).
- [35] Cameron Calcluth, Alessandro Ferraro, and Giulia Ferrini. “Vacuum provides quantum advantage to otherwise simulatable architectures”. *Phys. Rev. A* **107**, 062414 (2023).
- [36] Cameron Calcluth, Nicolas Reichel, Alessandro Ferraro, and Giulia Ferrini. “Sufficient condition for universal quantum computation using bosonic circuits”. *PRX Quantum* **5**, 020337 (2024).
- [37] Ulysse Chabaud and Mattia Walschaers. “Resources for bosonic quantum computational advantage”. *Phys. Rev. Lett.* **130**, 090602 (2023).
- [38] Ulysse Chabaud, Roohollah Ghobadi, Salman Beigi, and Saleh Rahimi-Keshari. “Phase-space negativity as a computational resource for quantum kernel methods” (2024). [arXiv:2405.12378](https://arxiv.org/abs/2405.12378).
- [39] Kevin E Cahill and Roy J Glauber. “Ordered expansions in boson amplitude operators”. *Physical Review* **177**, 1857 (1969).
- [40] N. Lütkenhaus and Stephen M. Barnett. “Nonclassical effects in phase space”. *Phys. Rev. A* **51**, 3340–3342 (1995).
- [41] Ching Tsung Lee. “Measure of the nonclassicality of nonclassical states”. *Physical Review A* **44**, R2775 (1991).
- [42] Seth Lloyd and Samuel L. Braunstein. “Quantum computation over continuous variables”. *Phys. Rev. Lett.* **82**, 1784–1787 (1999).
- [43] Timo Hillmann, Fernando Quijandría, Göran Johansson, Alessandro Ferraro, Simone Gasparinetti, and Giulia Ferrini. “Universal gate set for continuous-variable quantum computation with microwave circuits”. *Phys. Rev. Lett.* **125**, 160501 (2020).
- [44] Hakop Pashayan, Joel J Wallman, and Stephen D Bartlett. “Estimating outcome probabilities of quantum circuits using quasiprobabilities”. *Physical Review Letters* **115**, 070501 (2015).
- [45] Daniel Gottesman, Alexei Kitaev, and John Preskill. “Encoding a qubit in an oscillator”. *Physical Review A* **64**, 012310 (2001).
- [46] Mile Gu, Christian Weedbrook, Nicolas C. Menicucci, Timothy C. Ralph, and Peter van Loock. “Quantum computing with continuous-variable clusters”. *Phys. Rev. A* **79**, 062318 (2009).
- [47] Youngrong Lim and Changhun Oh. “Approximating outcome probabilities of linear optical circuits”. *npj Quantum Information* **9**, 124 (2023).
- [48] Ulysse Chabaud, Roohollah Ghobadi, Salman Beigi, and Saleh Rahimi-Keshari. “Phase-space negativity as a computational resource for quantum kernel methods” (2024). [arXiv:2405.12378](https://arxiv.org/abs/2405.12378).

A Explicit calculations for eq. (13)

Similarly to its construction for operators, it is possible to construct ordered quasiprobability distributions for quantum channels (see e.g. [20]). Figure 2 illustrates a generic quantum process; the simulation task would amount to sampling from $p(\mathbf{n}) = \text{Tr}[\rho_{out}\Pi_{\mathbf{n}}]$. It is possible to rewrite this probability distribution in terms of (\mathbf{s})-ordered quasi-probability distributions using a generalization of the trace rules for Wigner functions [39]: for any two bounded operators O_1, O_2 of trace class we can write

$$\text{Tr}[O_1 O_2] = \int_{\xi \in \mathbb{C}} \frac{d^{2M}\xi}{\pi^M} W_{O_1}^{(-s)} W_{O_2}^{(s)}. \quad (32)$$

Thus leading to

$$p(\mathbf{x}) = \text{Tr}[\rho_{out}\hat{\Pi}_{\mathbf{x}}] = \int_{\beta \in \mathbb{C}} \pi^{2M} d^{2M}\beta W_{\hat{\Pi}_{\mathbf{x}}}^{(-s)}(\beta) W_{\rho_{out}}^{(s)}(\beta), \quad (33)$$

where

$$W_{\hat{\Pi}_{\mathbf{x}}}^{(-s)}(\beta) = \int_{\xi \in \mathbb{C}} \pi^{-2M} d^{2M}\xi \text{Tr}[\Pi_{\mathbf{n}} D(\xi, -s)] e^{\beta\xi^\dagger - \xi\beta^\dagger} \quad (34)$$

and

$$W_{\rho_{out}}^{(s)}(\beta) = \int_{\xi \in \mathbb{C}} \pi^{-2M} d^{2M}\xi \chi_{\rho_{out}}^{(s)}(\xi) e^{\beta\xi^\dagger - \xi\beta^\dagger}. \quad (35)$$

One can write the M modes input state in terms of displacement operators as

$$\rho_{in} = \int_{\mathbf{x}, \mathbf{i} \in \mathbb{C}} \chi_{\rho_{in}}^{(s')}(\xi) e^{-\xi s' \xi^\dagger / 2} D^\dagger(\xi) \frac{d^{2M}\xi}{\pi^M}. \quad (36)$$

This implies, by linearity of the quantum process, that the output state is

$$\rho_{out} = \int_{\xi \in \mathbb{C}} \chi_{\rho_{in}}^{(s')}(\xi) e^{-\xi s' \xi^\dagger / 2} \mathcal{E}(D^\dagger(\xi)). \quad (37)$$

Moreover, by virtue of the inverse Fourier transform, the (\mathbf{s})-ordered characteristic function of the output state is

$$\chi_{\rho_{out}}^{(s)}(\zeta) = \text{Tr}[\rho_{out} D(\zeta, s)] \quad (38)$$

By plugging eq. (37) into the last we find

$$\chi_{\rho_{out}}^{(s)}(\zeta) = \int_{\xi \in \mathbb{C}} \chi_{\rho_{in}}^{(s')}(\xi) \text{Tr}[\mathcal{E}(D^\dagger(\xi, s')) D(\zeta, s)] \frac{d^{2M}\xi}{\pi^M} \quad (39)$$

Which can be re-written in terms of the (\mathbf{s}')-ordered Wigner function of the input state

$$\chi_{\rho_{out}}^{(s)}(\zeta) = \int_{\xi \in \mathbb{C}} d^{2M}\xi \int_{\alpha \in \mathbb{C}} d^{2M}\beta W_{\rho_{in}}^{(s')}(\beta) \text{Tr}[\mathcal{E}(D^\dagger(\xi, s')) D(\zeta, s)]. \quad (40)$$

Using the Fourier transform we can find a relation between the input and output ordered Wigner functions,

$$W_{\rho_{out}}^{(s)}(\beta) = \int_{\alpha \in \mathbb{C}} d^{2M}\alpha W_{\rho_{in}}^{(s')}(\alpha) \Lambda_{\mathcal{E}}^{(-s', s)}(\alpha, \beta) \quad (41)$$

where we define the (\mathbf{s}', \mathbf{s})-ordered transfer function $\Lambda_{\mathcal{E}}^{(s', s)}(\alpha, \beta)$ as

$$\Lambda_{\mathcal{E}}^{(s', s)}(\alpha, \beta) = \int_{\zeta \in \mathbb{C}} d^{2M}\zeta \int_{\xi \in \mathbb{C}} d^{2M}\xi e^{\beta\xi^\dagger - \xi\beta^\dagger + \xi\alpha^\dagger - \alpha\xi^\dagger} e^{\zeta s \zeta^\dagger / 2 + \xi s' \xi^\dagger / 2} \text{Tr}[\mathcal{E}(D^\dagger(\xi)) D(\zeta)]. \quad (42)$$

Finally, by plugging last equation into eq. (33) we find the highlighted result of [20]:

$$p(\mathbf{x}) = \iint_{\alpha, \beta \in \mathbb{C}} \pi^M d^{2M}\alpha d^{2M}\beta W_{\rho_{in}}^{(s')}(\alpha) \Lambda_{\mathcal{E}}^{(-s', s)}(\alpha, \beta) W_{\hat{\Pi}_{\mathbf{x}}}^{(-s)}(\beta) \quad (43)$$

The last step needed to find eq. (13) is to replace \mathcal{E} by a sequence of trace-preserving quantum channels $\mathcal{E}_1 \circ \mathcal{E}_2 \circ \dots \circ \mathcal{E}_k$ and notice that

$$\Lambda_{\mathcal{E}_1 \circ \mathcal{E}_2}^{(-s', s)}(\alpha, \beta) = \int_{\gamma \in \mathbb{C}} \Lambda_{\mathcal{E}_1}^{(-s', s'')}(\alpha, \gamma) \Lambda_{\mathcal{E}_2}^{(-s'', s)}(\gamma, \beta) \quad (44)$$

Leading naturally to eq. (13).

These functions are all defined on the complex plane, rather than on the real symplectic phase-space that is commonly encountered when dealing with Wigner functions. To convert to quadrature notation, one can use the following identities:

$$\begin{cases} \hat{q} = \hat{a} + \hat{a}^\dagger, & \hat{p} = -i(\hat{a} - \hat{a}^\dagger) \\ \vec{q} = \frac{\xi + \xi^\dagger}{2}, & \vec{p} = \frac{\xi - \xi^\dagger}{2i} \end{cases} \quad (45)$$

B Explicit calculations for the cubic gate

Let $\hat{U}_\gamma = \exp(-i\frac{\gamma}{3!}\hat{q}^3)$. Firstly, we need to compute the characteristic function of this gate:

$$\text{Tr} \left[\hat{U}_\gamma D^\dagger(\xi) \hat{U}_\gamma^\dagger D(\zeta) \right] \quad (46)$$

It is convenient to start by rewriting $D(\xi)$ in terms of the real, quadratures variables:

$$D(\xi) = \exp\{\xi\hat{a}^\dagger - \xi^*\hat{a}\} = \exp\{-i(q_1\hat{p} - p_1\hat{q})\} \quad (47)$$

We have that $\hat{U}_\gamma\hat{q}\hat{U}_\gamma^\dagger = \hat{q}$, while $\hat{U}_\gamma\hat{p}\hat{U}_\gamma^\dagger = \hat{p} + \gamma\hat{q}^2$, from which it follows that:

$$\hat{U}_\gamma D^\dagger(\xi) \hat{U}_\gamma^\dagger = \exp\{-i[q_1(\hat{p} + \gamma\hat{q}^2) - p_1\hat{q}]\} \quad (48)$$

where $q_1 = \text{Re}\xi$ and $p_1 = \text{Im}\xi$. To compute the trace using the eigenbasis of \hat{q} , it is useful to rearrange this result as:

$$\exp\{-i[q_1(\hat{p} + \gamma\hat{q}^2) - p_1\hat{q}]\} = e^{a\hat{p}} e^{b\hat{q} + c\hat{q}^2 + d} \quad (49)$$

for a proper choice of $a, b, c \in \mathbb{C}$. Notice that there must be a solution, since commutators of quadratic operators in the quadratures form a closed subalgebra and a term in \hat{p}^2 cannot appear, as it is not present in the exponent on the left-hand side. We can compute a, b, c by applying the Baker-Campbell-Hausdorff formula to the right-hand side, to get:

$$\begin{aligned} & e^{a\hat{p}} e^{b\hat{q} + c\hat{q}^2} \\ &= \exp\left\{a\hat{p} + b\hat{q} + c\hat{q}^2 + \frac{1}{2}[a\hat{p}, b\hat{q} + c\hat{q}^2] + \dots\right\} \\ &= \exp\left\{a\hat{p} + (b - 2iac)\hat{q} + c\hat{q}^2 - iab + \frac{1}{12}[a\hat{p}, -2iac\hat{q}]\right\} \\ &= \exp\left\{a\hat{p} + (b - 2iac)\hat{q} + c\hat{q}^2 - iab - \frac{1}{3}a^2c\right\} \end{aligned} \quad (50)$$

and we used $[\hat{q}, \hat{p}] = 2i$. All higher order commutators vanish, since the last second-order nested commutator is a scalar. By direct comparison with the left-hand side of eq. (49) we conclude that:

$$\begin{aligned} a &= -iq_1, & c &= -iq_1\gamma \\ b &= ip_1 - 2iq_1^2\gamma, & d &= iq_1p_1 - \frac{5}{3}i\gamma q_1^3 \end{aligned} \quad (51)$$

If we similarly rewrite $D(\zeta) = e^{iq_2p_2} e^{iq_2\hat{p}} e^{-ip_2\hat{q}}$, with $q_2 = \text{Re}\zeta$ and $p_2 = \text{Im}\zeta$, we finally have:

$$\begin{aligned} & \text{Tr} \left[\hat{U}_\gamma D^\dagger(\xi) \hat{U}_\gamma^\dagger D(\zeta) \right] = \\ &= e^\phi \int_{q \in \mathbb{R}} dq \langle q | e^{a\hat{p}} e^{b\hat{q} + c\hat{q}^2} e^{iq_2\hat{p}} e^{-ip_2\hat{q}} | q \rangle = \\ &= e^\phi \int_{q \in \mathbb{R}} dq e^{-ip_2q} \langle q - 2q_1 | e^{b\hat{q} + c\hat{q}^2} | q - 2q_2 \rangle = \\ &= e^\phi \delta(q_1 - q_2) \int_{q \in \mathbb{R}} dq e^{-ip_2q + b(q - 2q_1) + c(q - 2q_1)^2} = \\ &= e^{\tilde{\phi}} \delta(q_1 - q_2) \int_{q \in \mathbb{R}} dq e^{i(p_1 - p_2 - 2\gamma q_1^2)q - i\gamma q_1 q^2} \end{aligned} \quad (52)$$

with $\phi = i(q_1 p_1 + q_2 p_2) - \frac{5}{3} i \gamma q_1^3$ and $\tilde{\phi} = i q_1 (p_1 - p_2) - \frac{5}{3} i \gamma q_1^3$. The remaining integration is the Fourier transform of a Gaussian with an imaginary variance, and it can be computed by regularising the integral, to find:

$$\int_{q \in \mathbb{R}} dq e^{i(p_1 - p_2 - 2\gamma q_1^2)q - i\gamma q_1 q^2} = \sqrt{\frac{\pi}{i\gamma q_1}} e^{i \frac{(p_1 - p_2 - 2\gamma q_1^2)^2}{4\gamma q_1}} \quad (53)$$

Putting everything together, we arrive at:

$$\text{Tr} \left[\hat{U}_\gamma D^\dagger(\xi) \hat{U}_\gamma^\dagger D(\zeta) \right] = \delta(q_1 - q_2) \sqrt{\frac{\pi}{i\gamma q_1}} e^{-\frac{(p_1 - p_2)^2}{4i\gamma q_1} - \frac{2}{3} i\gamma q_1^3} \quad (54)$$

The next steps consist in performing the Fourier transform of this function with respect to q_1, q_2, p_1, p_2 , with additional Gaussian weights that impose the (s_1, s_2) ordering, that is, multiplying the result of eq. (54) by:

$$e^{\alpha^* \xi - \alpha \xi^* + \beta \zeta^* - \beta^* \zeta} e^{\frac{s_1 |\xi|^2}{2} + \frac{s_2 |\zeta|^2}{2}} = \exp[2i(q_\alpha p_1 - p_\alpha q_1 + p_\beta q_2 - q_\beta p_2)] \exp\left[\frac{s_1}{2}(q_1^2 + p_1^2) + \frac{s_2}{2}(q_2^2 + p_2^2)\right] \quad (55)$$

Because of the delta distribution, the integration with respect to q_2 is trivial. Also, the integrations with respect to p_1 and p_2 amounts to computing the Fourier transform of Gaussian functions with complex variance; these converge if and only if the real part of the variance is positive, such that the integrand decays exponentially in p_1 and p_2 . Also, observing that the Gaussian factor in $\text{Tr} \left[\hat{U}_\gamma D^\dagger(\xi) \hat{U}_\gamma^\dagger D(\zeta) \right]$ is purely imaginary, the conditions of convergence are just $s_1 < 0$ and $s_2 < 0$. The general formula that should be applied for the integrations in p_1 and p_2 is then:

$$\forall A, B \in \mathbb{C} : \text{Re}(A) > 0 \quad \implies \quad \int_{x \in \mathbb{R}} e^{-Ax^2 + iBx} dx = \sqrt{\frac{\pi}{A}} e^{-\frac{B^2}{4A}} \quad (56)$$

and the end result is:

$$2 \int_{q_1 \in \mathbb{R}} dq_1 \sqrt{\frac{2\pi^3}{-(s_1 + s_2) + 2i\gamma q_1 s_1 s_2}} \times \exp\left[2 \frac{-(q_\alpha + q_\beta)^2 + 2i\gamma q_1 (s_1 q_\alpha^2 + s_2 q_\beta^2)}{-(s_1 + s_2) + 2i\gamma q_1 s_1 s_2} + \frac{s_1 + s_2}{2} q_1^2 - \frac{2}{3} i\gamma q_1^3 - 2i(p_\alpha - p_\beta)q_1\right] \quad (57)$$

Again, for $s_1, s_2 \leq 0$ the integral must converge. Notice, moreover, that the integrand is Gaussian in q_α, q_β and the real part of the variance is positive as long as $s_1, s_2 < 0$. Finally, it depends only upon the combination $p_\alpha - p_\beta$ and not on the single variables independently. We can then conclude that $\Lambda_{\hat{U}_\gamma}^{(s_1, s_2)}(q_\alpha, p_\alpha, q_\beta, p_\beta)$ is a well-defined function whenever $s_1, s_2 < 0$ and we should now find the function $S(s_1)$ such that $\Lambda_{\hat{U}_\gamma}^{(s_1, s_2)}$ is also positive semidefinite if and only if $s_2 < S(s_1)$. Given the highly oscillatory behaviour of the complex-valued function to be integrated, this is far from an easy task. We can first try to compute the proper Wigner function by computing the limits $s_1 \rightarrow 0^-, s_2 \rightarrow 0^-$ and noticing that:

$$\lim_{s_1, s_2 \rightarrow 0^-} \sqrt{\frac{1}{-(s_1 + s_2) + 2i\gamma q_1 s_1 s_2}} \exp\left[2 \frac{-(q_\alpha + q_\beta)^2 + 2i\gamma q_1 (s_1 q_\alpha^2 + s_2 q_\beta^2)}{-(s_1 + s_2) + 2i\gamma q_1 s_1 s_2}\right] = \sqrt{\frac{\pi}{2}} \delta(q_\alpha + q_\beta) \quad (58)$$

while

$$\int_{q_1 \in \mathbb{R}} dq_1 \exp\left[-\frac{2}{3} i\gamma q_1^3 - 2ipq_1\right] = \pi \left(\frac{4}{\gamma}\right)^{1/3} \text{Ai}\left(\frac{p}{2^{-2/3}\gamma^{1/3}}\right) \quad (59)$$

where

$$\text{Ai}(x) = \frac{1}{\pi} \int_0^{+\infty} \cos\left(\frac{t^3}{3} + xt\right) dt$$

is the standard Airy function. Putting everything together we find:

$$\Lambda_{\hat{U}_\gamma}^{(0,0)}(q_\alpha, p_\alpha, q_\beta, p_\beta) = 2\pi^3 \delta(q_\alpha + q_\beta) \left(\frac{4}{\gamma}\right)^{1/3} \text{Ai}\left(\frac{p_\alpha - p_\beta}{2^{-2/3}\gamma^{1/3}}\right) \quad (60)$$

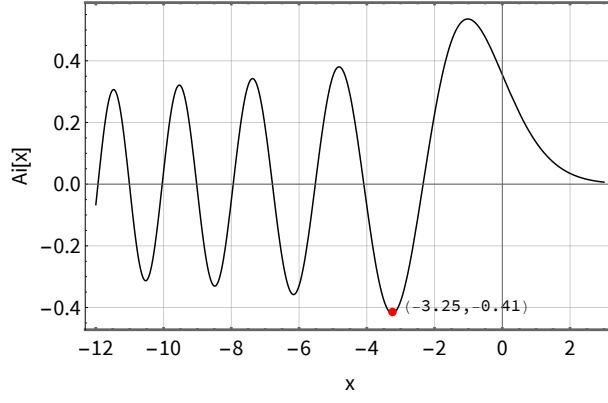


Figure B5: The Airy function $\text{Ai}(x)$ in the range $x \in [-12, 3]$.

Finally, for generic $s_1, s_2 < 0$, we can apply eq. (4):

$$\begin{aligned} \Lambda_{\hat{U}_\gamma}^{(s_1, s_2)}(q_\alpha, p_\alpha, q_\beta, p_\beta) &= \frac{4}{s_1 s_2 \pi^4} \int_{\tilde{q}_\alpha, \tilde{p}_\alpha, \tilde{q}_\beta, \tilde{p}_\beta \in \mathbb{R}} d\tilde{q}_\alpha d\tilde{p}_\alpha d\tilde{q}_\beta d\tilde{p}_\beta \\ &\times \exp \left[2 \frac{(q_\alpha - \tilde{q}_\alpha)^2 + (p_\alpha - \tilde{p}_\alpha)^2}{s_1} + 2 \frac{(q_\beta - \tilde{q}_\beta)^2 + (p_\beta - \tilde{p}_\beta)^2}{s_2} \right] \Lambda_{\hat{U}_\gamma}^{(0,0)}(\tilde{q}_\alpha, \tilde{p}_\alpha, \tilde{q}_\beta, \tilde{p}_\beta) \end{aligned} \quad (61)$$

The integrations in \tilde{q}_α and \tilde{q}_β are easily done thanks to the delta and the fact that the remaining integral is Gaussian:

$$\begin{aligned} \Lambda_{\hat{U}_\gamma}^{(s_1, s_2)}(q_\alpha, p_\alpha, q_\beta, p_\beta) &= 4 \sqrt{\frac{2}{-\pi(s_1 + s_2)s_1 s_2}} \left(\frac{4}{\gamma}\right)^{1/3} e^{\frac{2}{s_1 + s_2}(q_\alpha - q_\beta)^2} \times \\ &\times \int_{\tilde{p}_\beta \in \mathbb{R}} d\tilde{p}_\beta \int_{\tilde{p}_\alpha \in \mathbb{R}} d\tilde{p}_\alpha \exp \left[2 \frac{(p_\alpha - \tilde{p}_\alpha)^2}{s_1} + 2 \frac{(p_\beta - \tilde{p}_\beta)^2}{s_2} \right] \text{Ai} \left(\frac{\tilde{p}_\alpha - \tilde{p}_\beta}{2^{-2/3}\gamma^{1/3}} \right) \end{aligned} \quad (62)$$

Performing the substitution $z = \tilde{p}_\alpha - \tilde{p}_\beta$ with respect to the integration in \tilde{p}_α and then exchanging the integration order, we can solve one more integral in \tilde{p}_β as a Gaussian integral:

$$\int_{\tilde{p}_\beta \in \mathbb{R}} d\tilde{p}_\beta \exp \left[2 \frac{(p_\alpha - z - \tilde{p}_\beta)^2}{s_1} + 2 \frac{(p_\beta - \tilde{p}_\beta)^2}{s_2} \right] = \sqrt{\frac{\pi}{2}} \sqrt{\frac{s_1 s_2}{-(s_1 + s_2)}} \exp \left[2 \frac{(z - p_\alpha + p_\beta)^2}{s_1 + s_2} \right] \quad (63)$$

to arrive at the following final expression:

$$\begin{aligned} \Lambda_{\hat{U}_\gamma}^{(s_1, s_2)}(q_\alpha, p_\alpha, q_\beta, p_\beta) &= \frac{4}{-(s_1 + s_2)} \left(\frac{4}{\gamma}\right)^{1/3} \exp \left[\frac{2(q_\alpha - q_\beta)^2}{s_1 + s_2} \right] \\ &\times \int_{z \in \mathbb{R}} dz \exp \left[\frac{2(z - p)^2}{s_1 + s_2} \right] \text{Ai} \left(\frac{z}{2^{-2/3}\gamma^{1/3}} \right) \end{aligned} \quad (64)$$

Again, it depends only on the combination $p = p_\alpha - p_\beta$ of the two momentum-like quadratures and it is invariant under the exchange of s_1 and s_2 . The sign of this function is clearly determined just by the sign of the last integral, and we should therefore determine when this integral can attain negative values in p . To this end, let us perform the substitution $y = z/(2^{-2/3}\gamma^{1/3})$ and rename $w = p/(2^{-2/3}\gamma^{1/3})$ to write²:

$$\mathcal{I}(r, w) = \int_{y \in \mathbb{R}} dy \exp \left[-\frac{(y - w)^2}{r} \right] \text{Ai}(y) \quad (65)$$

with $r = -(s_1 + s_2)2^{-1/3}\gamma^{-1/3}$ being the only relevant combination of s_1, s_2 and γ . We finally need to determine whether there exists a value of $r > 0$ such that $\mathcal{I}(r, w) \geq 0 \forall w \in \mathbb{R}$.

In fig. B5 we show the plot of the Airy function $\text{Ai}(x)$, whose absolute minimum occurs around $\tilde{x} \simeq -3.24820$. For small values of r , the Gaussian will be narrow and we can expect that the value of w for which $\mathcal{I}(r, w)$ is the lowest will be close to \tilde{x} . In this regime, the function will indeed attain negative values for w close to \tilde{x} , therefore we can conclude that whenever $|s_1 + s_2| \ll 2^{1/3}\gamma^{1/3}$ the cubic gate cannot be represented by a

²We omit the positive prefactor in front, assuming $\gamma > 0$ without loss of generality

non-negative transfer function. In particular, since $-1 \leq s_1, s_2 \leq 0$, this is always the case if $\gamma > 4$. The problem is numerically unstable, since modest changes in r around $r \simeq 10$ make the values of the minimum of $\mathcal{I}(r, w)$ with respect to w oscillate around zero with orders of magnitude smaller than 10^{-10} . To give some sensible bounds, we verified that that $\min_w \mathcal{I}(r, w) \geq -1. * 10^{-2}$ for $r \geq 5.5$, $\min_w \mathcal{I}(r, w) \geq -1. * 10^{-3}$ for $r \geq 7.38$ and $\min_w \mathcal{I}(r, w) \geq -1. * 10^{-4}$ for $r \geq 8.7$. Calling $r^*(\epsilon)$ the smallest value of r such that $\forall r \geq r^*(\epsilon) : \min_w \mathcal{I}(r, w) > -\epsilon$, with $0 < \epsilon \ll 1$, one can numerically derive a series of bounds of the form:

$$s_2 \leq -s_1 - 2^{1/3} \gamma^{1/3} r^*(\epsilon) \quad (66)$$

From which it is clear that the relation between the output and input parameter is linear and with coefficient -1 for any γ .